# MAGNETIC EFFECTS ON SURFACE WAVES IN A ROTATING NON-HOMOGENEOUS HALF-SPACE WITH GROOVED AND IMPEDANCE BOUNDARY CHARACTERISTICS

A.I. ANYA[*]

GST- Mathematics Division, Veritas University Abuja, NIGERIA
E-mail: anyaa@veritas.edu.ng

C. NWACHIOMA

Department of Mechanical Engineering, University of Colorado Denver, USA

H. ALI

Department of Mathematics, Faculty of Science, COMSATS University Islamabad, PAKISTAN

Mathematical modeling of waves in a rotating grooved and impedance boundary of a non-homogeneous fibre-reinforced solid half-space under the influence of a magnetic field and mechanical force is investigated. We derived analytically, the dynamical equations for the rotating grooved and impedance boundary of the non-homogeneous fibre-reinforced solid under the influence of magnetic fields and mechanical force. Harmonic solution method of wave analysis is utilized. The components of displacements and stresses are developed and studied after employing dimensionless parameters in the equations of motion. Numerical computations are presented in a graphical form by using Mathematica Software for a particular chosen material. We observed that the combined grooved, magnetic fields, impedance boundary and other physical parameters, have remarkable effects on the material. A decrease in horizontal impedance yielded maximum amplitudes of displacements and stresses of the waves on the fibre-reinforced medium. The mechanical force and rotation of the medium induced increased behaviors to the amplitudes of displacement and stress components of the wave on the solid medium. Thus, this work should be of great importance in studies involving seismology and seismic mechatronic solutions for stress-wave generation in non-homogeneous materials.

Key words: magnetic fields, non-homogeneous half space, rotation, grooved and impedance boundary, mechanical force.

## 1. Introduction

Mechanical waves are associated with solid mechanics of materials and in particular with elastodynamics. They need a medium to propagate and hence do not travel via free space. However, the assumptions of only isotropic features in a solid medium may not give accurate characteristics of the continuum responses linked to composites, geophysical materials, mechatronics devices, etc. Thus, studies in solid mechanics have always involved the need to find suitable ways in interpreting disturbances in these media. Research on solid mechanics is particularly useful in the fields of mechatronics, geomechanics, civil engineering, structural designing, and geology, amongst others. This has paved way for materials that are anisotropic in nature rather than isotropic. One of these anisotropic materials is a composite material. It is obvious that composite materials show self-reinforced behaviors under some given pressure or temperature conditions. The mechanical behavior of composite materials can also well be understood via the studies of anisotropic elasticity like the fibre-reinforced composite materials (Spencer, [1]). Fibre reinforced medium tends to be similar to another important type of material known as an orthotropic material; which could be considered in the investigation of elastodynamic models. Thus, in describing the propagation of waves in

---

[*] To whom correspondence should be addressed

such materials, mathematical models are usually made handy along with some given physical properties and parameters such as rotation of the medium and magnetic fields (Schoenberg *et al.* [2] and Abd-Alla *et al.* [3]). A magnetic field is a vector field that prescribes the magnetic influences on moving charges and magnetic materials and this could result in a pull or push.

In spite of this, impedance boundary conditions are a linear combination of unknown functions and their derivatives prescribed on the boundary (Singh, [6]). These are commonly used in various fields of physics like electromagneto-acoustics phenomena.

Furthermore, boundary surfaces of some materials are plane, grooved/corrugated or entirely of different shapes in nature. A grooved boundary surface could be visualized as a series of parallel furrows and ridges whose occurrence in mechanical propagation of wave results in several effects, especially across interfaces (Asano, [4]). Interestingly, some authors made contributions to this concept of corrugated boundary and other related wave propagation phenomena (Singh, *et al.* [9-11]; Das *et al.* [12]; Abd-Alla *et al.* [13]; Chattopadhyay *et al.* [14]; Roy *et al.* [16]; Singh *et al.* [17]; Gupta *et al.* [18-19]; Anya *et al.* [20-23]; [24]; Maleki *et al.* [24], Chowdhury *et al.* [25]; Singh *et al.* [26-27]; [28]; Sahu *et al.* [28], Giovannini, [29] and Rakshit *et al.* [30-31]).

This article is aimed at developing a mathematical model to study waves on a rotating grooved and impedance boundary of a non-homogeneous fibre-reinforced solid half-space under the influence of a magnetic field and mechanical force. The dynamic equations are derived by incorporating these physical properties of rotation, magnetism and non-homogeneity of the material as well as employing dimensionless parameters to the equations of motion. Normal mode analysis was adopted in finding solutions to the equations of motion. And by using grooved and impedance boundary conditions with an underlying mechanical force, a complete solution to the displacement components and stresses of the wave on the material were analytically and graphically developed and presented for a chosen material. We observed that these parameters have remarkable effects on the component of displacements of the waves and stresses on the medium in a 2D space analysis.

## 2. The mathematical model and formulations

The constitutive relations for a fibre-reinforced elastic anisotropic solid [1] and magnetic force [2] are given:

$$
\tau_{ij} = \lambda \varepsilon_{kk} \delta_{ij} + 2\mu_T \varepsilon_{ij} + \alpha \left( a_k a_m \varepsilon_{km} \delta_{ij} + \varepsilon_{kk} a_i a_j \right) +
$$
$$
+ 2\left( \mu_L - \mu_T \right)\left( a_i a_k \varepsilon_{kj} + a_j a_k \varepsilon_{ki} \right) + \beta \left( a_k a_m \varepsilon_{km} a_i a_j \right),
\tag{2.1}
$$

$$
F_i = \mu_0 H_0^2 \left( e_{,1} - \varepsilon_0 \mu_0 \ddot{u}_1, \ e_{,2} - \varepsilon_0 \mu_0 \ddot{u}_2, \ 0 \right), \quad i = 1,2,3,
\tag{2.2}
$$

for

$$
\varepsilon_{ij} = \tfrac{1}{2}\left( u_{i,j} + u_{j,i} \right) \quad \text{and} \quad h_i = \left( 0, \ 0, -e \right)
$$

where $e = u_{i,i}$, $i = i, 2$.

Here $\tau_{ij}, \varepsilon_{ij}, u_i, \delta_{ij}, \lambda, (\alpha, \beta, (\mu_L - \mu_T))$ and $F_i$ are the stress tensor, strain tensor, displacement vector, Kronecker-delta function, Lames constant, fiber-reinforced parameters and magnetic force respectively. We take $a = (a_1, a_2, a_3)$ such that $a = (1,0,0)$ represents the fibre directions:

$$
H_i = H_0 \delta_{i3} + h_i
$$

where $h_i$ is the induced magnetic field, $\varepsilon_o$ is the electric permeability and the material lies in the $x_1 x_2 -$ plane:

$$h_i\left(x_1, x_2, x_3\right) = -u_{k,k}\delta_{i3}.$$

When $H_i$ is the magnetic vector field and $\mu_o$ is the magnetic permeability from Maxwell's equations of electromagnetism.

In the presence of magnetic fields and rotation of the media [3], the field equation follows:

$$\tau_{ij,j} + F_i = \rho\left\{\ddot{u}_i + \Omega_j u_j \Omega_i - \Omega^2 u_i + 2\varepsilon_{ijk}\Omega_j \dot{u}_k\right\} \tag{2.3}$$

where $\varepsilon_{jim}$ is the Levi-Civita tensor and the given index after comma connotes partial derivatives with respect to the coordinate space and the superscript dot stipulates partial derivative with respect to time. Consider the deformation in the $x_1 x_2-$ plane such that $x_3 = 0$ and $x_1 \neq x_2 \neq 0$ and the displacements $u_1 \neq u_2 \neq u_3 \neq 0$. We also assume the rotation $\Omega = \Omega(0,0,1)$, i.e. the rotation of the media is about the $x_3$-axis. Make on assumption that the non-homogeneity grows or decays slowly and that its rate of growth or decay is proportional to its value. In the present problem, we consider an exponentially decaying non-homogeneous fibre-rinforced material. Hence density, elastic modulus and elastic parameters are taken in the following form [5]; [8]:

$$\left(\alpha, \beta, \lambda, \mu_T, \mu_L, \rho\right) = \left(\alpha_0, \beta_0, \lambda_0, \mu_{T_0}, \mu_{L0}, \rho_0\right)e^{-mx_2},$$

here $m$ is the non-homogeneous parameter.

In view of the fact that the tensors are symmetric, Eq.(2.3) in component forms with the consideration of the non-homogeneity of the medium becomes:

$$\begin{aligned}&\left(\lambda + 2\alpha + 4\mu_L - 2\mu_T + \beta + \mu_0 H_0^2\right)u_{1,11} + \left(\alpha + \lambda + \mu_L + \mu_0 H_0^2\right)u_{2,21} + \mu_L u_{1,22} -\\&+ m\mu_T\left(u_{1,2} + u_{2,1}\right) = \left\{\rho + \varepsilon_0\mu_0^2 H_0^2\right\}\ddot{u}_1 + \rho\left\{-\Omega^2 u_1 - 2\Omega\dot{u}_2\right\},\end{aligned} \tag{2.4}$$

$$\begin{aligned}&\left(\alpha + \lambda + \mu_L + \mu_0 H_0^2\right)u_{1,12} + \mu_L u_{2,11} + \left(\lambda + 2\mu_T + \mu_0 H_0^2\right)u_{2,22} - m\left(\lambda + \alpha\right)u_{1,1} +\\&- m\left(\lambda + 2\mu_T\right)u_{2,2} = \left\{\rho + \varepsilon_0\mu_0^2 H_0^2\right\}\ddot{u}_2 + \rho\left\{-\Omega^2 u_2 + 2\Omega\dot{u}_1\right\},\end{aligned} \tag{2.5}$$

$$\mu_L u_{3,11} + \mu_T u_{3,22} - m\mu_T u_{3,2} = \rho\ddot{u}_3. \tag{2.6}$$

Equations (2.4)-(2.6) can be rewritten as:

$$A_1 u_{1,11} + A_2 u_{2,21} + A_3 u_{1,22} - mA_4\left(u_{1,2} + u_{2,1}\right) = \left\{\rho + \varepsilon_0\mu_0^2 H_0^2\right\}\ddot{u}_1 + \rho\left\{-\Omega^2 u_1 - 2\Omega\dot{u}_2\right\}, \tag{2.7}$$

$$A_2 u_{1,12} + A_3 u_{2,11} + A_5 u_{2,22} - mA_6 u_{1,1} - mA_7 u_{2,2} = \left\{\rho + \varepsilon_0\mu_0^2 H_0^2\right\}\ddot{u}_2 + \rho\left\{-\Omega^2 u_2 + 2\Omega\dot{u}_1\right\}, \tag{2.8}$$

$$A_3 u_{3,11} + A_4 u_{3,22} - mA_4 u_{3,2} = \rho\ddot{u}_3 \tag{2.9}$$

where

$$A_1 = \left(\lambda + 2\alpha + 4\mu_L - 2\mu_T + \beta + \mu_0 H_0^2\right), \quad A_2 = \left(\alpha + \lambda + \mu_L + \mu_0 H_0^2\right), \quad A_3 = \mu_L,$$

$$A_4 = \mu_T, \quad A_5 = \left(\lambda + 2\mu_T + \mu_0 H_0^2\right), \quad A_6 = (\lambda + \alpha), \quad A_7 = (\lambda + 2\mu_T).$$

For convenience, we consider the following dimensionless constants:

$$\left(x_1', x_2', u_1', u_2'\right) = c_0 \left(x_1, x_2, u_1, u_2\right), \quad \left(t'\right) = c_0^2 t, \quad \Omega' = \Omega / c_0^2, \quad \sigma_{ij}' = \sigma_{ij} / \rho c_0^2, \quad c_0^2 = A_1 / \rho.$$

Introducing the dimensionless constants above into Eqs (2.7)-(2.9) and by dropping the upper sign " $'$ ", gives:

$$u_{1,11} + A_{12} u_{2,21} + A_{13} u_{1,22} - m A_{24} \left(u_{1,2} + u_{2,1}\right) =$$
$$= \left\{\left(1 + \varepsilon_0 \mu_0^2 H_0^2 / \rho\right) \ddot{u}_1 - \rho \Omega^2 u_1 - 2\rho \Omega \dot{u}_2\right\}, \tag{2.10}$$

$$A_{12} u_{1,12} + A_{13} u_{2,11} + A_{15} u_{2,22} - m A_{26} u_{1,1} - m A_{27} u_{2,2} =$$
$$= \left\{\left(1 + \varepsilon_0 \mu_0^2 H_0^2 / \rho\right) \ddot{u}_2 - \rho \Omega^2 u_2 + 2\rho \Omega \dot{u}_1\right\}, \tag{2.11}$$

$$A_{13} u_{3,11} + A_{14} u_{3,22} - m A_{24} u_{3,2} = \ddot{u}_3 \tag{2.12}$$

where

$$\left(A_{12}, A_{13}, A_{14}, A_{15}, A_{16}, A_{17}\right) = \left(A_2, A_3, A_4, A_5, A_6, A_7\right) / A_1$$

and

$$\left(A_{24}, A_{26}, A_{27}\right) = \left(A_{14}, A_{16}, A_{17}\right) \rho^{1/2} / A_1^{3/2}.$$

## 3. Analytical solution of the problem

In this section, consider a rotating grooved and impedance boundary of a non-homogeneous magneto-elastic fibre-reinforced solid in the half-space $x_2 < 0$ subjected to mechanical force. Let the normal mode approach be adopted such that the waves have the displacements taken as:

$$u_j = (\overline{u}_j(x_2)) e^{\omega t + i b x_1}, \quad j = 1, 2, 3. \tag{3.1}$$

Introducing Eq.(3.1) into the set of Eqs (2.10-2.12), we obtained:

$$\left\{A_{13} D^2 - m A_{24} D - b^2 - \left(1 + \varepsilon_0 \mu_0^2 H_0^2 / \rho\right) \omega^2 + \rho \Omega^2\right\} \overline{u}_1 +$$
$$+ \left(i A_{12} b D - m A_{24} b i - 2\rho \Omega \omega\right) \overline{u}_2 = 0, \tag{3.2}$$

$$\left(i A_{12} b D - m b i A_{26} + 2\rho \Omega \omega\right) \overline{u}_1 +$$
$$+ \left\{A_{15} D^2 - m A_{27} D - A_{13} b^2 - \left(1 + \varepsilon_0 \mu_0^2 H_0^2 / \rho\right)\right) \omega^2 + \rho \Omega^2\right\} \overline{u}_2 = 0, \tag{3.3}$$

$$\left\{ A_{14}D^2 - mA_{24}D - \left( A_{13}b^2 + \rho\omega^2 \right) \right\} \overline{u}_3 = 0. \tag{3.4}$$

A non- trivial solution to the set of homogenous linear Eqs (3.2)-(3.3) becomes the quartic equation below. For a homogenous medium, this will result to a quadratic homogenous characteristic equation in $D^2$.

$$\left( C_1 D^4 + C_2 D^3 + C_3 D^2 + C_4 D + C_5 \right) \left( \overline{u}_1, \overline{u}_2 \right) = 0 \tag{3.5}$$

where $C_i$, $i = 1, 2, 3, 4, 5$ are complex coefficients which depend upon the material parameters. Given that $v_i$, $i = 1, 2, 3, 4$ be positive real roots of the characteristics or auxiliary Eq.(3.5), normal mode approach implies we have the following form of solution

$$\left( \overline{u}_1, \overline{u}_2 \right) = \sum_{n=1}^{4} \left( N_n, N_{1n} \right) e^{-v_n x_2} \tag{3.6}$$

where $N_n$ and $N_{1n}$ are undoubtedly parameters which depends upon the wave number $b$ in the $x_1$ direction and the complex frequency $\omega$ of the waves. We introduce Eq.(3.6) into Eqs (2.10)-(2.11) and obtain the relations:

$$N_{1n} = H_{1n}N_n \tag{3.7}$$

where

$$H_{1n} = \frac{\left\{ A_{13}v_n^2 + mA_{24}v_n - b^2 - \left( 1 + \varepsilon_0\mu_0^2 H_0^2 / \rho \right)\omega^2 + \rho\Omega^2 \right\} - \left( 2\rho\Omega\omega - iA_{12}bv_n - mbiA_{26} \right)}{\left\{ A_{15}v_n^2 - A_{13}b^2 + mA_{27}v_n - \left( 1 + \varepsilon_0\mu_0^2 H_0^2 / \rho \right)\omega^2 + \rho\Omega^2 \right\} + \left( 2\rho\Omega\omega + iA_{12}bv_n + mbiA_{24} \right)}$$

$$n = 1, 2, 3, 4.$$

The uncoupled Eq (3.4) has the solution:

$$u_3 = \left( Ze^{-\ell_1 x_2} + Z_1 e^{\ell_2 x_2} \right) e^{\omega t + ibx_1}. \tag{3.8}$$

That is $\ell_{1,2} = 1 / 2 \left\{ mA_{24} / A_{14} \pm \left[ \left( mA_{24} / A_{14} \right)^2 + 4 \left( A_{13}b^2 + \rho\omega^2 \right) / A_{14} \right]^{1/2} \right\}$ represents the roots of the uncoupled equation. Considering the existence of transverse components and boundedness of solution, the uncoupled Eq.(3.4) takes the form; $u_3 = Ze^{-\ell_1 x_2 + \omega t + ibx_1}$. The solutions for the total displacement component functions and stresses on the material in the dimensionless forms are thus obtained:

$$u_1 = \sum_{n=1}^{4} N_n e^{-v_n x_2 + \omega t + ibx_1}, \quad u_2 = \sum_{n=1}^{4} N_n H_{1n} e^{-v_n x_2 + \omega t + ibx_1}, \quad u_3 = Ze^{-\ell_1 x_2 + \omega t + ibx_1},$$

$$\tau_{11} = \sum_{n=1}^{4} \left\{ ib \left[ 1 - \left( \mu_0 H_0^2 / A_1 \right) \right] - v_n H_{1n} A_{16} \right\} N_n e^{-(v_n + m)x_2 + \omega t + ibx_1},$$

$$\tau_{22} = \sum_{n=1}^{4} \{ibA_{16} - \nu_n H_{1n} A_{17}\} N_n e^{-(\nu_n + m)x_2 + \omega t + ibx_1},$$

$$\tau_{12} = \sum_{n=1}^{4} (ibH_{1n} - \nu_n) A_{13} N_n e^{-(\nu_n + m)x_2 + \omega t + ibx_1},$$

$$\tau_{21} = \sum_{n=1}^{4} A_{13} (ibH_{1n} - \nu_n) N_n e^{-(\nu_n + m)x_2 + \omega t + ibx_1},$$

$$\tau_{23} = \sum_{n=1}^{4} \{-\nu_n A_{14} Z\} N_n e^{-(\ell_n + m)x_2 + \omega t + ibx_1}.$$

## 4. Grooved and impedance boundary conditions and applications

Suppose the equation of grooved boundary of the fibre-reinforced half-space is denoted $x_2 = \eta(x_1)$, where $\eta(x_1)$ is a periodic function and independent of $x_3$. Assuming a suitable origin of spaces, trigonometric Fourier series of $\eta(x_1)$ can be represented as follows [4]:

$$\eta(x_1) = \sum_{l=1}^{\infty} \left( \eta_l e^{ilbx_1} + \eta_{-l} e^{-ilbx_1} \right), \tag{4.1}$$

where $\eta_l$ and $\eta_{-l}$ are Fourier expansion coefficients and $l$, is the series expansion order. Let us introduce the constants $a$, $F_l$ and $I_l$ as follows: $\eta_l^{\pm} = a/2$, $\eta_l^{\pm} = (F_l + I_l)/2$, $l = 2,3...$, and

$$\eta(x_1) = a\cos bx_1 + F_2 \cos 2bx_1 + I_2 \sin 2bx_1 + ... + F_l \cos lbx_1 + I_l \sin lbx_1,$$

where $F_l$ and $I_l$ are the Fourier cosine and sine coefficients, respectively. It suffices that the nature of the grooved or corrugated boundary surface can be denoted with the help of cosine terms, that is, $\eta(x_1) = a\cos bx_1$, where $a$ is the amplitude of the grooved boundary and $b$ is the wavenumber associated with the grooved boundary surface such that the grooved boundary possesses the wavelength $2\pi/b$.

    i.   The components of displacements for the coupled equations at the surface take the form:
        $u_1 = 0$, and $u_2 = 0$, at $x_2 = \eta(x_1)$, for all $x_1$ and $t$

    ii.  Stress with respect to $x_2 = \eta(x_1)$ for the coupled equations takes the form:

$$\tau_{22} - \eta'(x_1)\tau_{21} + \overline{\tau}_{ij} + \omega Z_{12} u_2 = P e^{\omega t + ibx_1},$$
$$\tau_{12} - \eta'(x_1)\tau_{11} + \omega Z_{11} u_1 = 0, \text{ for all } x_1 \text{ and } t.$$

    iii. Boundary conditions for the uncoupled equation become

        $u_3 = 0$, and $\tau_{23} = 0$, at $x_2 = \eta(x_1)$, for all $x_1$ and $t$.

Here, $\overline{\tau}_{ij} = \mu_0 H_0 \begin{bmatrix} -h_3 & 0 & h_1 \\ 0 & -h_3 & h_2 \\ h_1 & h_2 & h_3 \end{bmatrix}$ [2]. Thus, we have that:

$$h_3 = -H_0(u_{1,1} + u_{2,2}), \quad h_1 = h_2 = 0 \quad \text{and} \quad \tau_{22} + \overline{\tau}_{22} = 0 \Rightarrow \tau_{22} + \mu_0 H_0^2 (u_{1,1} + u_{2,2}) = 0.$$

The shear stress which is the tangential stress component $\tau_{12}$ and normal stress component $\tau_{22}$ are proportional to tangential and normal displacement components and time frequency, respectively. However, involving the grooved boundary conditions of the material and the mechanical force $P_1$ [7], yielded (ii). $Z_1$ and $Z_2$ are the proportional coefficients called impedance parameters. We can recover the traction free boundary conditions if $P_1 = 0$. Note that $P = P_1 e^{-mx_2}$, $Z_{11} = Z_1 e^{-mx_2}$, $Z_{12} = Z_2 e^{-mx_2}$. Applying the boundary conditions for the coupled equations, we obtain:

$$N_n = 0, \tag{4.2}$$

$$H_{1n} N_n = 0, \tag{4.3}$$

$$\begin{aligned}
&(ibA_{16} - \nu_n H_{1n} A_{17}) e^{-\nu_n \eta(x_1)} N_n + ab \sin bx_1 \{(ibH_{1n} - \nu_n) A_{13}\} e^{-\nu_n \eta(x_1)} N_n + \\
&+ \{\omega H_{1n} Z_2 N_n + \mu_0 H_0^2 (ib - \nu_n H_{1n})\} e^{-\nu_n \eta(x_1)} N_n = P_1,
\end{aligned} \tag{4.4}$$

$$(ibH_{1n} - \nu_n) A_{13} N_n + ab \sin bx_1 \left\{ ib\left[1 - (\mu_0 H_0^2 / A_1)\right] - \nu_n H_{1n} A_{16} \right\} N_n + (\omega Z_1) N_n = 0. \tag{4.5}$$

$$n = 1, 2, 3, 4.$$

The above system of Eqs (4.2-4.5) gives the values for the complete solutions to the displacement components of the waves and stresses (normal and shear stresses) on the material in view of the physical parameters considered when $N_n, n = 1, 2, 3, 4$ are solved for. A novel dispersion relations of waves in a rotating non-homogeneous half space with grooved and impedance boundary characteristics influenced by magnetic fields is also achieved or obtained for the complete model if we eliminate $N_n, n = 1, 2, 3, 4$ from Eqs (4.2)-(4.5) and for a nontrivial solution of the non-homogeneous system of equations.

## 5. Numerical computation and analysis

This section affords us the opportunity in utilizing the numerical fiber-reinforced physical constants [15] and other given parameters below to ascertain the behavioral tendencies of the rotating non-homogenous material in terms of its normal and shear stresses, and component of displacements occasioned by effects of the grooved and impedance boundary, magnetic fields, and mechanical force parameters on the material as the wave propagates. Thus, following solutions to the dimensionless boundary and dynamical equations as presented in this paper the analyses of the various effects of these parameters are graphically presented in Figs. 1-9, below.

$$\mu_T = 2.46 \times 10^{10} \, kg \, m^{-1} s^{-2}, \quad \mu_L = 5.66 \times 10^{10} \, kg \, m^{-1} s^{-2}, \quad \lambda = 5.65 \times 10^{10} \, kg \, m^{-1} s^{-2},$$

$$\rho = 2660 kg \, m^{-3}, \quad \alpha = -1.28 \times 10^{10} \, kg \, m^{-1} s^{-2}, \quad \beta = 220.9 \times 10^{10} \, kg \, m^{-1} s^{-2},$$

$$\omega = (2+i) \, rad/s, \quad H_0 = 500 A/m, \quad t = 9s, \quad b = 0.6, \quad m = 0.40, \quad \Omega = 10 rad/s$$

$$a = 0.29, \quad P_1 = 1N, \quad Z_1 = 0.5 \quad Z_2 = 0.7, \quad x_1 = 1.3m.$$

Figure 1 shows the effects of the displacement $u_i$, $i = 1, 2$, normal stress $\tau_{22}$ and shear stress $\tau_{12}$ components versus $x_2$ for varying time $t$ in seconds with constant parameters of magnetic fields $H_0$, mechanical force $P_1$, non-homogenous parameter $m$, rotation of the medium $\Omega$, impedance and grooved boundary $Z_i$, $i = 1, 2$ and $a$, $b$ respectively. The displacement components and stresses showed an outright decrease in behaviors when the time $t$ for which the wave is on the material is increased. The maxima for the displacements and stresses on the material tend to be achieved for a given small quantity of time $t$. This stipulates that with the considered parameters and varying time $t$ (in a decrease sense of it), the wave on the material would cause a greater impact and with good amount of the material covered. This shows a physical assertion where the reinforcement of the material has yielded a positive result and when the wave is presumed to propagate longer on the material as it shows vanishing effects across the length of the material. Thus, impact on the material for shorter time provides higher amplitudes as the wave hits the surface of the material and tends to be controlled with lesser effects and amplitudes as it propagates across the length of the material.
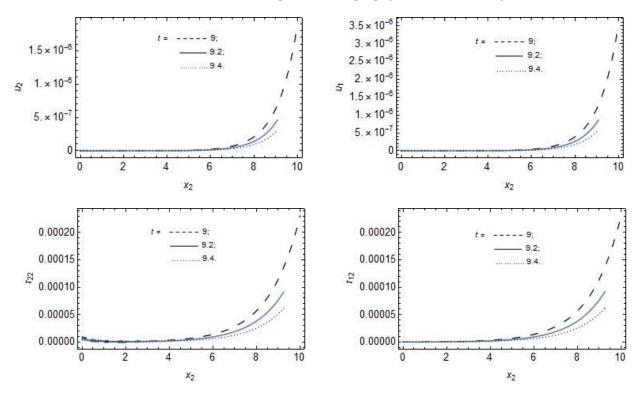


Fig.1. Variations of the displacement components $u_i$, $i = 1, 2$, normal stress $\tau_{22}$ and shear stress $\tau_{12}$ versus $x_2$ in meters for distinct time $t$ in seconds.

Figure 2 illustrates the variations of the displacement components $u_i$, $i = 1, 2$, normal stress $\tau_{22}$ and shear stress $\tau_{12}$ against $x_2$ for distinct amplitudes $a$ of the grooved boundary with constant parameters of magnetic fields $H_0$, mechanical force $P_1$, rotation of the medium $\Omega$, non-homogenous parameter $m$, impedance and wave number of the grooved boundary; $Z_i$, $i = 1, 2$ and $b$ respectively and with time $t$ in seconds. It shows that the grooved parameter $a$ caused a decrease in the displacement of the waves as well as the stresses on the material when increased. The maximum displacement components or stresses are attained for a small amount of the amplitude of the grooved boundary with respect to the considered parameters. Physically, high amplitudes of the grooved boundary would yield more vanishing effects to the normal displacements and stress components and the normal stress components $\tau_{22}$ having mixed behaviors for $x_2 \geq 6$ and $a = 0.49, 0.69$.
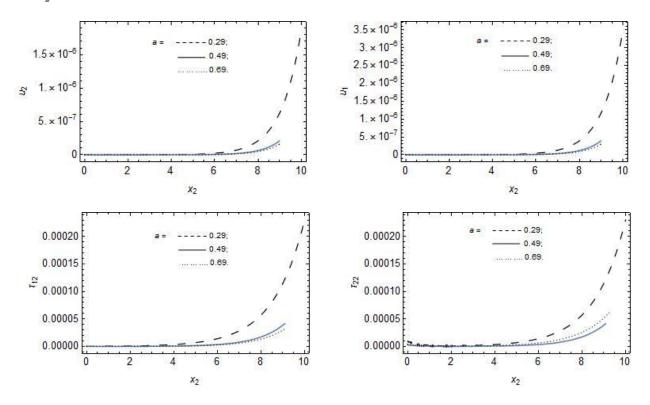


Fig.2. Variations of the displacement components $u_i$, $i = 1, 2$, normal stress $\tau_{22}$ and shear stress $\tau_{12}$ versus $x_2$ in meters for distinct values of the grooved parameter $a$.

Consequently, Fig.3 shows the variations of the displacement components $u_i$, $i = 1, 2$, normal stress $\tau_{22}$ and shear stress $\tau_{12}$ versus $x_2$ for a varying wave number $b$ of the grooved boundary with constant parameters of magnetic fields $H_0$, non-homogenous parameter $m$, mechanical force $P_1$, rotation of the medium $\Omega$, impedance and amplitude of the grooved boundary $Z_i$, $i = 1, 2$ and $a$, respectively and with time $t$. We observe that the wave number of the grooved parameter $b$ caused increased behaviors of the displacements and stresses on the material as the wave propagates. The maximum displacements and stresses are attained for an increased grooved boundary parameter $b$ with respect to the other considered parameters. The displacements and stresses tend to vanish faster for $x_2 \geq 8$, $b = 0.8$ after attaining maximum.
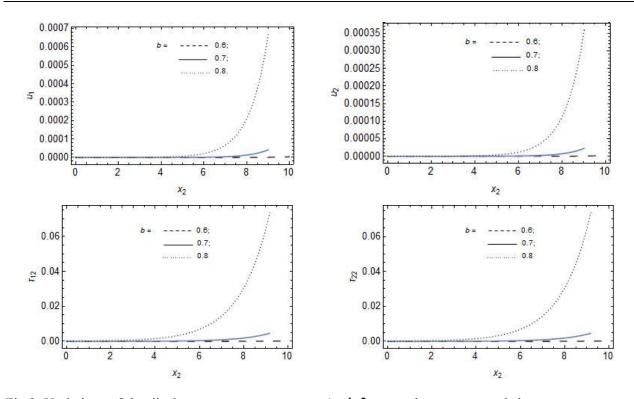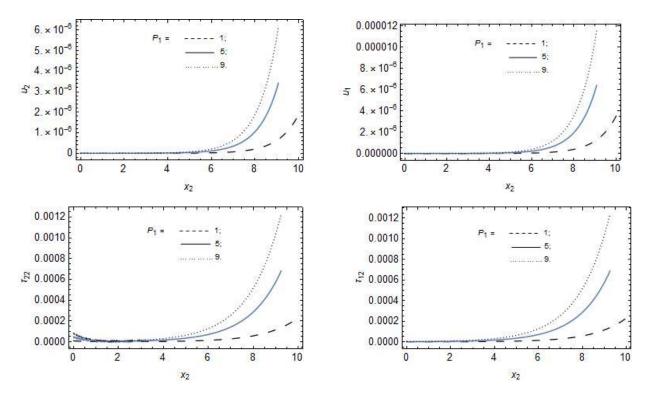
Fig.3. Variations of the displacement components $u_i$, $i = 1, 2$, normal stress $\tau_{22}$ and shear stress $\tau_{12}$ versus $x_2$ in meters for distinct values of the grooved parameter $b$.



Fig.4. Variations of the displacement components $u_i$, $i = 1, 2$, normal stress $\tau_{22}$ and shear stress $\tau_{12}$ versus $x_2$ in meters for distinct values mechanical force $P_1$ in Newton.

Figure 4 gives the variations of the displacement components $u_i$, $i = 1, 2$, and stresses $\tau_{22}$ and $\tau_{12}$ versus $x_2$ for a varying mechanical force $P_1$ with constant parameters of magnetic fields $H_0$, non-homogenous parameter $m$, rotation of the medium $\Omega$, impedance and grooved boundary parameters $Z_i$, $i = 1, 2$ and $a, b$, respectively at a given time $t$. Increase in the mechanical force shows that the displacements and stresses on the material with respect to the considered parameters increases. Also, we observe that this increase in mechanical force could lead to the vanishing of the wave on the material as it propagates across the material and more especially after attaining its maximum. Thus it suffices to say that the maximum amplitudes would be achieved for an increased mechanical force $P_1$ on the fibre-reinforced material. This is a phenomenon of a push to the material characteristics thereby adding more force to the wave modulations.

In spite of this, Fig.5 shows the effects on the displacement components $u_i$, $i = 1, 2$, and stresses $\tau_{22}$ and $\tau_{12}$ versus $x_2$ for distinct magnetic fields $H_0$ with constant parameters of the mechanical force $P_1$, rotation of the medium $\Omega$, non-homogenous parameter $m$, impedance and grooved boundary parameters $Z_i$, $i = 1, 2$ and $a, b$, respectively at a given time $t$. Thus, we deduced that an increase in the amount of magnetic fields tend to constantly cause a mixed behavior of the displacement components and stresses on the fibre-reinforced material. However, the maximum amplitude of displacement and stresses are respectively attained in all cases when there is a high magnetic force on the material with respect to the considered parameters. Physically, this has exerted a push on the displacements and stresses on the material.
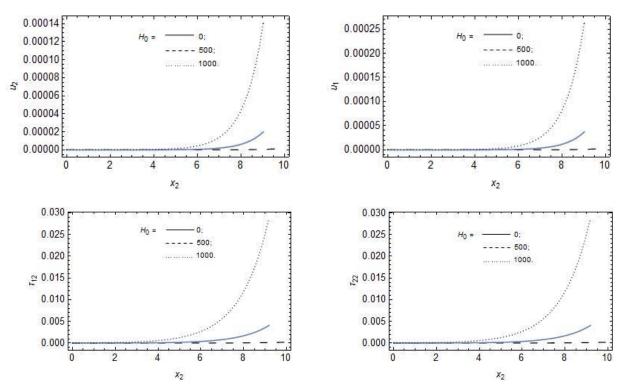


Fig.5. Variations of the displacement components $u_i$, $i = 1, 2$, normal stress $\tau_{22}$ and shear stress $\tau_{12}$ versus $x_2$ in meters for distinct values of $H_0 A / m$.

Furthermore, Fig.6 describes the effects on the displacement components $u_i$, $i = 1, 2$, and stresses $\tau_{22}$ and $\tau_{12}$ against $x_2$ for a distinct non-homogenous parameter $m$ with constant parameters of the mechanical force $P_1$, rotation of the medium $\Omega$, magnetic fields $H_0$, impedance and grooved boundary

parameters $Z_i$, $i = 1, 2$ and $a,b$, respectively, at a given time $t$. Thus, an increase in the non-homogenous parameter shows a gradual increase of the displacements and stresses on the material. As the material deforms, there is a supposedly gradual malleability or change in state and properties of the medium and hence a rise in displacement and stresses applied by the waves propagating on the material. The maximum amplitude of displacement and stresses on the material is achieved for a small or negligible non-homogeneity of the material.
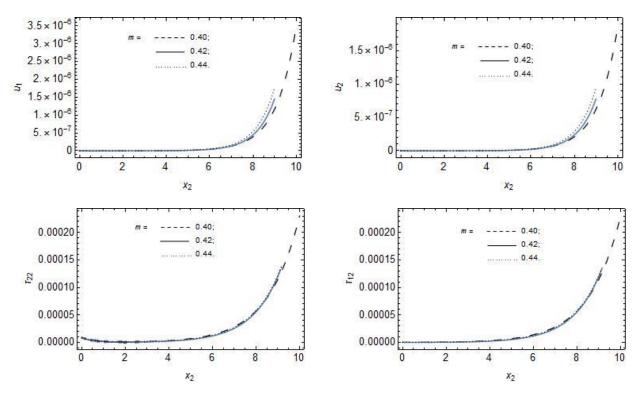


Fig.6. Variations of the displacement components $u_i$, $i = 1, 2$, normal stress $\tau_{22}$ and shear stress $\tau_{12}$ versus $x_2$ in meters for distinct values of the non-homogenous parameter $m$.

Figure 7 demonstrates the effects of the displacement components $u_i$, $i = 1, 2$, and stresses $\tau_{22}$ and $\tau_{12}$ against $x_2$ for distinct rotation of the medium $\Omega$ with constant parameters of the mechanical force $P_1$, magnetic fields $H_0$, non-homogenous parameter $m$, impedance and grooved boundary parameters $Z_i$, $i = 1, 2$ and $a,b$, respectively, at a given time $t$. Deductions made from Fig.7 suggest an increase in behaviors of the displacements and stress components on the material for an increased in rotation of the medium. The maximum displacement and stresses on the material tend to be attained when the rotation of the medium increases and for $x_2 = 9$ where vanishing effects of the wave are ignited at $\Omega = 10.2$.

Figure 8 shows the effects of the displacement components $u_i$, $i = 1, 2$, stresses $\tau_{22}$ and $\tau_{12}$ against $x_2$ for distinct impedance $Z_2$ with constant parameters of the mechanical force $P_1$, magnetic fields $H_0$, rotation of the medium $\Omega$, non-homogenous parameter $m$, impedance and grooved boundary parameters $Z_1$ and $a,b$, respectively, at a given time $t$. We found out that an increase in the impedance $Z_2$ led to a gradual increase to the components of the displacements and stress on the material and that it vanishes faster as expected along the coordinates due impedance. Also, observe that the maximum amplitude of displacements and stresses of waves are obtained for an increased vertical or normal impedance $Z_2$ on the material.
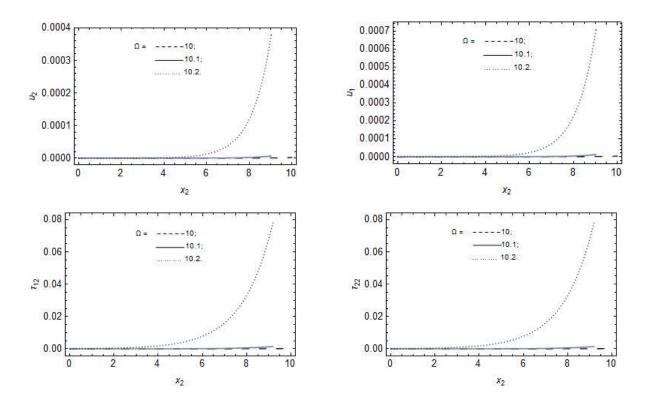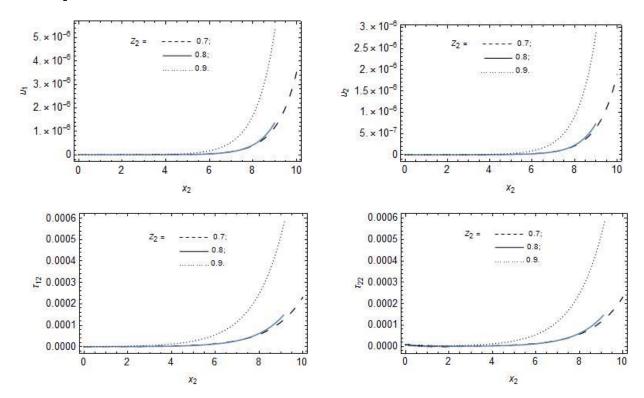
Fig.7. Variations of the displacement components $u_i$, $i = 1, 2$, normal stress $\tau_{22}$ and shear stress $\tau_{12}$ versus $x_2$ in meters for distinct values of the rotation $\Omega$ *rad / s* of the media.

Fig.8. Variations of the displacement components $u_i$, $i = 1, 2$, normal stress $\tau_{22}$ and shear stress $\tau_{12}$ versus $x_2$ in meters for distinct values of impedance $Z_2$.

Figure 9 shows the effects of the displacement components $u_i$, $i = 1, 2$, stresses $\tau_{22}$ and $\tau_{12}$ against $x_2$ for distinct impedance $Z_1$ with constant parameters of the mechanical force $P_1$, magnetic fields $H_0$, rotation of the medium $\Omega$, non-homogenous parameter $m$, impedance and grooved boundary parameters $Z_2$ and $a,b$, respectively, at a given time $t$ are presented. We found out that an increase in the impedance $Z_1$ produces a near reluctance decrease to the components of the displacement and stresses on the material. Also, observe that a decrease in the impedance $Z_1$ yields maximum displacements and stresses of the waves on the fibre-reinforced medium whilst physically entailing a compelling surface mechanical resistance to the surface waves on the material.
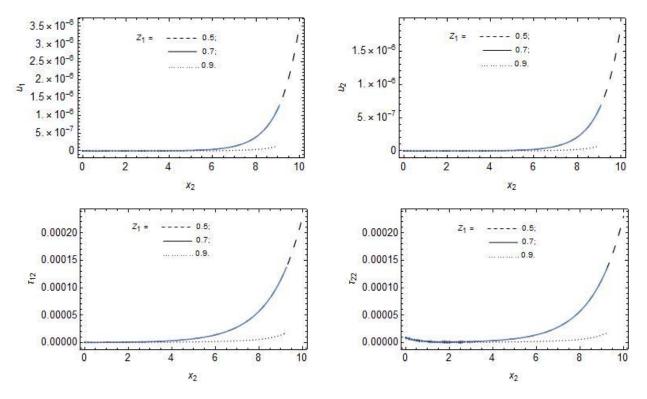


Fig.9. Variations of the displacement components $u_i$, $i = 1, 2$, normal stress $\tau_{22}$ and shear stress $\tau_{12}$ versus $x_2$ in meters for distinct values of $Z_1$.

## 6. Conclusion

This paper has successfully dealt with the study of mathematical modelling of waves associated with a rotating non-homogeneous fibre-reinforced medium under the influence of a magnetic field and mechanical force with characteristics of grooved and impedance boundary. The components of displacements and stresses were derived in view of the dimensionless parameters in the dynamical equations by utilizing the normal mode solution approach. A novel dispersion relation of the model was given. Graphical presentations were made in order to examine the effects of these contributing physical phenomena of the mechanical force $P_1$, magnetic fields $H_0$, rotation of the medium $\Omega$, non-homogeneity $m$, impedance and grooved boundary parameters at a given time $t$. We observed that the combined contributing parameters have an enormous effect on the displacements and stresses of the wave on the material. The conclusions are as follows:

- Mixed behaviors for an increase in magnetic fields on the medium were deduced. High magnetic effects produced or showed somewhat high amplitudes of displacement and stress components on the material.
- Also, a decrease in the horizontal components of the impedance yielded maximum displacements and stresses of the waves on the fibre-reinforced medium.
- Increasing the amount of rotation of the media and mechanical force tends to constantly cause an increase in the displacement components and stresses on the fibre-reinforced material.
- The grooved boundary parameters equally had their unique effects on the waves on the material. Amplitude of the grooved boundary *a*, caused a decrease of the displacement of the waves as well as the stresses on the material when increased while the reverse is the case for the wave number associated with the grooved boundary.
- Non-homogeneity of the material showed a gradual increase in the amplitudes of the displacement and stress components of the wave on the material.
- Increase in the mechanical force shows that the displacements and stresses on the material with respect to the considered parameters do increase.

## Nomenclatures

$\tau_{ij}$ – stress tensor.

$\varepsilon_{ij}$ – strain tensor.

$u_i$ – displacement vector.

$\delta_{ij}$ – Kronecker-delta function.

$\lambda$ – Lame's constant.

$\alpha,\ \beta,\ (\mu_L - \mu_T)$ – fibre-reinforced parameters.

$F_i$ – magnetic force.

$\varepsilon_o$ – electric permeability.

$\mu_o$ – magnetic permeability.

$H_i$ – magnetic vector field.

$\Omega$ – rotation.

$\rho$ – density

$x_i$ – coordinates.

$P_l$ – mechanical force.

$Z_1, Z_2$ – impedance parameters

## Appendix

$$C_1 = A_{13}A_{15}, \quad C_2 = -m\left(A_{15}A_{24} + A_{13}A_{27}\right),$$

$$C_3 = \left\{-b^2 i^2 \rho A_{12}^2 - b^2 \rho A_{15} - \rho \omega^2 A_{15} + \rho^2 \Omega^2 A_{15} + m^2 \rho A_{24} A_{27} - \right.$$
$$\left. + \omega^2 A_{15} H_0^2 \varepsilon_0 \mu_0^2 + A_{13}\left(-\rho \omega^2 + \rho^2 \Omega^2 - b^2 \rho A_{13} - \omega^2 H_0^2 \mu_0^2\right)\right\},$$

$$C_4 = \left\{m\left[b^2 i^2 \rho A_{12} A_{26} + A_{24}\left(\rho \omega^2 - \rho^2 \Omega^2 + b^2 i^2 \rho A_{12} + b^2 \rho A_{13} + \omega^2 H_0^2 \mu_0^2\right) + \right.\right.$$
$$\left.\left. + A_{27}\left(\rho\left(b^2 + \omega^2 - \rho \Omega^2\right) + \omega^2 H_0^2 \varepsilon_0 \mu_0^2\right)\right]\right\} / \rho,$$

$$C_5 = \frac{1}{\rho^2}\Big\{ b^2\rho^2\omega^2 + \rho^2\omega^4 - b^2\rho^3\Omega^2 - 2\rho^3\omega^2\Omega^2 + 4\rho^4\omega^2\Omega^2 + \rho^4\Omega^4 - 2bim\rho^3\omega\Omega A_{26} +$$

$$+ bim\rho^2 A_{24}\left(2\rho\omega\Omega - bimA_{26}\right) + b^2\rho\omega^2 H_0^2\mu_0^2 + \rho\omega^4 H_0^2\mu_0^2 - \rho^2\omega^2\Omega^2 H_0^2\mu_0^2 + \rho\omega^4 H_0^2\varepsilon_0\mu_0^2 -$$

$$+ \rho^2\omega^2\Omega^2 H_0^2\varepsilon_0\mu_0^2 + \omega^4 H_0^4\varepsilon_0\mu_0^4 + b^2\rho A_{13}\left(\rho\left(b^2 + \omega^2 - \rho\Omega^2\right) + \omega^2 H_0^2\varepsilon_0\mu_0^2\right)\Big\}.$$

# References

[1] Spencer A.J.M. (1972): *Deformations of Fibre-reinforced Materials*.– Oxford Uni. Pres. Lond.

[2] Abd-Alla A.M., Abo-Dahab, S.M. and Khan A. (2017): *Rotational effects on magneto- thermoelastic stonely, Love, and Rayleigh waves in fibre-reinforced anisotropic general viscoelastic media of higher order*.– CMC, vol.53, pp.49-72, https://doi.org/10.3970/cmc.2017.053.052

[3] Schoenberg M. and Censor D. (1973): *Elastic waves in rotating media*.– Quart. Appl. Math., vol.31, pp.115-125. DOI: 10.4236/am.2015.65075

[4] Asano S. (1966): *Reflection and refraction of elastic waves at a corrugated interface*.– Bull. Seism. Soc. Am., vol.56, pp.201-221

[5] Khan A., Anya A.I. and Kaneez H. (2015): *Gravitational effects on surface waves in non-homogeneous rotating fibre-reinforced anisotropic elastic media with voids.–* Int. J. Appl. Sci. Eng. Res.,vol.4, pp.620-632.

[6] Singh B. (2016): *Reflection of elastic waves from plane surface of a half-space with impedance boundary conditions.–* Geosci. Res., vol.2, pp.242-253.

[7] Ailawalia P., Sachdeva S.K. and Pathania D. (2015): *A two dimensional fibre reinforced micropolar thermoelastic problem for a half-space subjected to mechanical force.–* Theor. Appl. Mech., vol.42, pp.11-25, DOI:10.2298/TAM1501011A

[8] Munish S., Sharma A. and Sharma A. (2016): *Propagation of SH waves in a double non-homogeneous crustal layers of finite depth lying over an homogeneous half-space.–* Lat. Am. J. Solids Struct., vol.13, pp.2628-2642. https://doi.org/10.1590/1679-78253005

[9] Singh S.S. and Tomar S.K. (2008): *qP-wave at a corrugated interface between two dissimilar pre-stressed elastic half-spaces.–* J. Sound Vib., vol.317, No.3, pp.687-708.

[10] Singh A.K., Das A., Kumar S. and Chattopadhyay A. (2015): *Influence of corrugated boundary surfaces reinforcement, hydrostatic stress, heterogeneity and anisotropy on Love type wave propagation.–* Meccanica, vol.50, pp.2977-2994, doi:10.1007/s11012-015-0172-6

[11] Singh A.K., Mistri K.C. and Mukesh P.K. (2018): *Effect of loose bonding and corrugated boundary surface on propagation of Rayleigh-type wave.–* Lat. Am. J. Solids Struct., vol.15, doi.org/10.1590/1679-78253577

[12] Das S.C., Acharya D.P. and Sengupta D. R. (1992): *Surface waves in an inhomogeneous elastic medium under the influence of gravity.–* Rev. Roumaine Sci. Tech. Ser Mec. Appl., vol.37, pp.539-551.

[13] Abd-Alla A.M., Abo-Dahab S.M. and Alotaibi Hind A. (2016): *Effect of the rotation on a non-homogeneous infinite elastic cylinder of orthotropic material with magnetic field.–* J. Comput. Theor. Nanosci., vol.13, pp.4476-4492, doi:10.1166/jctn.2016.5308

[14] Chattopadhyay A. (1975): *On the dispersion equation for Love wave due to irregularity in the thickness of non-homogeneous crustal layer.–* Acta Geol. Pol., vol.23, pp.307-317.

[15] Sunita D., Suresh K.S. and Kapil K.K. (2019): *Reflection at the free surface of fibre-reinforced thermoelastic rotating medium with two temperature and* phase-lag.– Appl. Math. Model. vol.65, pp.106-119, https://doi.org/10.1016/j.apm.2018.08.004

[16] Roy I., Acharya D.P. and Acharya S. (2017): *Propagation and reflection of plane waves in a rotating magneto-elastic fibre-reinforced semi space with surface stress.–* Mech. & Mech. Eng., vol.21, pp.1043-1061, DOI:10.2478/mme-2018-0074

[17] Singh D. and Sindhu R. (2011): *Propagation of waves at interface between a liquid half- space and an orthotropic micropolar solid half-space.–* Adv. Acoust. & Vib., vol.2011, p.5, DOI:10.1155/2011/159437

[18] Gupta R.R. (2014): *Surface wave characteristics in a micropolar transversely isotropic half-space underlying an inviscid liquid layer.–* Int. J. of Appl. Mech. Eng., vol.19, pp.49-60.

[19] Gupta R.R. (2014): *Reflection of waves in a rotating transversely isotropic thermoelastic half-space under initial stress.–* J. of Solid Mech., vol.6, No.2, pp.229-239.

[20] Anya A.I., Akhtar M.W., Abo-Dahab M.S., Kaneez H., Khan A. and Adnan J. (2018): *Effects of a magnetic field and initial stress on reflection of SV-waves at a free surface with voids under gravity.–* J. Mech. Behav. Mater., vol.27, pp.56, https://doi.org/10.1515/jmbm-2018-0002

[21] Anya A.I. and Khan A. (2019): *Reflection and propagation of plane waves at free surfaces of a rotating micropolar fibre-reinforced medium with voids.–* Geomech. & Eng., vol.18, pp.605-614.

[22] Anya A.I. and Khan A. (2020): *Reflection and propagation of magneto-thermoelastic plane waves at free surfaces of a rotating micropolar fibre-reinforced medium under G-L theory.–* Int. J. of Acoust. and Vib., vol.25, pp.190-199, https://doi.org/10.20855/ijav.2020.25.21575

[23] Anya A.I. and Khan A. (2022): *Plane waves in a micropolar fibre-reinforced solid and liquid interface for non-insulated boundary under magneto-thermo-elasticity.–* J. Comput. Appl. Mech., vol. 53, pp.204-218, doi:10.22059/jcamech.2022.341656.712

[24] Maleki F. and Jafarzadeh F. (2023): *Model tests on determining the effect of various geometrical aspects on horizontal impedance function of surface footings.–* Scientia Iranica, in press, doi:10.24200/SCI.2023.59744.6403.

[25] Chowdhury S., Kundu S., Alam P. and Gupta Sh.(2021): *Dispersion of Stoneley waves through the irregular common interface of two hydrostatic stressed MTI medi.–* Scientia Iranica, vol.28, pp.837-846, doi:10.24200/SCI.2020.52653.2820.

[26] Singh B. and Kaur B.(2022): *Rayleigh surface wave at an impedance boundary of an incompressible micropolar solid half-spac.–* Mech. Adv. Mater. Struct., vol.29, No.25, pp.3942-3949 .

[27] Singh B. and Kaur B. (2020): *Rayleigh-type surface wave on a rotating orthotropic elastic half-space with impedance boundary conditions.–* J. Vib. Control, vol.26, pp.1980-1987.

[28] Sahu S.A., Mondal S. and Nirwal S. (2022): *Mathematical analysis of Rayleigh waves at the nonplanner boundary between orthotropic and micropolar media.–* Int. J. Geomech., vol.23, doi.org/10.1061/IJGNAI.GMENG-7246.

[29] Giovannini L.(2022): *Theory of dipole-exchange spin-wave propagation in periodically corrugated films.–* Phys. Rev. B, vol.105, doi.org/10.1103/PhysRevB.105.214426.

[30] Rakshit S., Mistri K.C., Das A. and Lakshman A. (2022): *Effect of interfacial imperfections on SH-wave propagation in a porous piezoelectric composit.–* Mech. Adv. Mater. Struct., vol.29, pp.4008-4018. doi.org/10.1080/15376494.2021.1916138.

[31] Rakshit S., Mistri K.C., Das A. and Lakshman A. (2021) *Stress analysis on the irregular surface of visco-porous piezoelectric half-space subjected to a moving load.–* J. Intell. Mater. Syst. Struct. vol.33, https://doi.org/10.1177/1045389X211048226.